MF, ZF, and MMSE filters for automotive OFDM radar

Bochra Benmeziane, Jean-Yves Baudais, Stéphane Méric, Kevin Cinglant

MF, ZF and MMSE filters for automotive OFDM radar

B. BENMEZIANE[1,2], J.-Y. BAUDAIS[1], S. MÉRIC[1] AND K. CINGLANT[2]

The delay estimation for OFDM automotive radars can be achieved through the use different filters. This paper compares two of these filters, namely the matched filter (MF) and the zero forcing filter (ZF) through two metrics which are the peak to sidelobe ratio (PSLR) and the integrated sidelobe ratio (ISLR) estimated on their range profiles. The analysis is then extended to the minimum mean squared error filter (MMSE).

Keywords: Radar signal processing, matched filter, zero forcing, minimum mean squared error, OFDM

I. INTRODUCTION

When it comes to automotive radars, one of the main issues is the increasing number of vehicles equipped with these radars threatening to saturate the band [5]. Many waveforms have been explored as substitutes to the current one such as Orthogonal Frequency Division Multiplexing (OFDM). OFDM is a multiplexing technique that uses orthogonal sub-carriers to transmit data [2]. This technique can be exploited for radar detection. Many filters can be exploited to estimate the delay induced by the distance of the target. Among these filters, our paper focuses on the matched filter (MF) and the zero forcing filter (ZF). The OFDM/MF radar estimates the delay through an autocorrelation function [3] and the OFDM/ZF radar estimates it through the impulse response of the channel [4].

The metrics used to compare these two filters are the peak to sidelobe ratio (PSLR) and the integrated sidelobe ratio (ISLR). These metrics are both crucial in automotive applications [5]. A high sidelobe might result in a false alarm, causing the vehicle to brake for no reason. Meanwhile, a high general level of sidelobes would raise the threshold above peaks linked to low power echos (farther targets). This would result in an equally dangerous effect. The two filters have been compared in [6] using the same metrics. This paper extends the analysis on the minimum mean squared error filter (MMSE) as a range estimation technique, and provides new and more accurate analytical derivations.

The article is organized as follows. Section II introduces the received echo and describes the range profiles for both OFDM/MF and OFDM/ZF. It also expresses the PSLR and ISLR for both filters and draws a link between the filters through these metrics. Section III extends the analysis to MMSE as a range estimation technique. Finally, section IV presents simulations to validate the findings.

[1]Univ Rennes, INSA Rennes, CNRS, IETR-UMR 6164, F-35000 Rennes, France
[2]ZF Autocruise, 760 avenue du Technopôle, 29280 Plouzané, France

II. RECEIVED SIGNAL WITH CONVENTIONAL FILTERS

The OFDM radar exploits orthogonal subcarriers to transmit data. It uses the inverse Fourier transform. An OFDM symbol is expressed as [8]

$$\forall t \in [0,T], x(t) = \frac{1}{\sqrt{N}} \sum_{n=0}^{N-1} a_n e^{\jmath 2\pi f_n t}, \qquad (1)$$

where f_n is the n^{th} subcarrier among a total sum of N subcarriers carrying a_n which is the n^{th} complex data symbol. The duration of the OFDM symbol is T with $f_n = \frac{n}{T}$. The cyclic prefix (CP) is added at the begining of the symbol to ensure the orthogonality of the subcarriers on the receiving end. The symbole from (1) becomes

$$\forall t \in [0,T+T_g], x(t) = \frac{1}{\sqrt{N}} \sum_{n=0}^{N-1} a_n e^{\jmath 2\pi f_n (t-T_g)}, \quad (2)$$

where T_g is the duration of the CP. The OFDM radar transmits a chain of OFDM symbols and the general expression of the signal is

$$\forall t \in \mathbb{R}, x(t) = \frac{1}{\sqrt{N}} \sum_{k=-\infty}^{+\infty} \sum_{n=0}^{N-1} a_{k,n} e^{\jmath 2\pi f_n (t-k(T+T_g)-T_g)}. \qquad (3)$$

The transmitted signal is

$$s(t) = x(t) e^{\jmath 2\pi f_c t}, \qquad (4)$$

where f_c is the carrier frequency and $a_{k,l}$ is the complex data symbol of the n^{th} subcarrier and the k^{th} OFDM symbol. The bandwidth used by the radar is $B = \frac{N}{T}$. The signal is assumed to be narrowband which means that $B \ll f_c$.

A target reflects the signal and the echo is received by the radar. The radial speed of the target is v and its range is $R(t) = R_0 + vt$ where R_0 is the initial range. The delay of

the echo is thus

$$\tau(t) = \frac{2(R_0 + vt)}{c} = \tau_0 + \frac{2v}{c}t, \tag{5}$$

where c is the speed of light and τ_0 is the delay of the echo due to the range of the target at the beginning of the duration of the symbol. We assume that $\frac{v}{c} \ll 1$. The received and mixed echo is

$$\begin{aligned} y(t) &= Ae^{\jmath\varphi}s(t-\tau(t))e^{-\jmath 2\pi f_c t} \\ &= Ae^{\jmath\varphi}x(t-\tau(t))e^{-\jmath 2\pi f_c \tau(t)} + w(t), \end{aligned} \tag{6}$$

with $w(t)$ a white Gaussian noise, and $Ae^{\jmath\varphi}$ the complex amplitude that takes into account the antenna gains, the RF chain, the path loss and the radar cross-section of the target. For the sake of simplicity, this amplitude is assumed to be $Ae^{\jmath\varphi} = 1$. In this scenario, it is assumed that the variation of $\tau(t)$ through the interval $t \in [k(T+T_g)+Tg, (k+1)(T+T_g)]$ is negligible. The delay of the kth OFDM symbol is thus $\tau_k = \tau(k(T+T_g)+Tg)$.

In what follows, we make the assumption that T_g is properly sized which means $\forall k, 0 \leq \tau_k < T_g \leq T$. The payload of the k^{th} echo is within the interval $[k(T+T_g)+Tg, (k+1)(T+T_g)]$. Let t' be the time within this interval, where $t = k(T+T_g)+T_g+t'$. The k^{th} echo becomes

$$y_k(t') = \frac{1}{\sqrt{N}}\sum_{n=0}^{N-1} a_{k,n}e^{\jmath 2\pi f_n(t'-\tau_k)}e^{-\jmath 2\pi f_c\tau_k} + w_k(t'). \tag{7}$$

The received echo is sampled with a sampling period of $T_s = \frac{T}{N}$. The sampled echo is

$$\begin{aligned} y[k,m] = &\frac{1}{\sqrt{N}}\sum_{n=0}^{N-1} a_{k,n}e^{\jmath 2\pi \frac{n}{T}(\frac{mT}{N}-\tau_k)}e^{-\jmath 2\pi f_c\tau_k} \\ &+ w[k,m]. \end{aligned} \tag{8}$$

Let $\phi_k = -2\pi f_c\tau_k$. The echo is OFDM demodulated through a Fourier transform and is expressed in the frequency domain as

$$\begin{aligned} Y[k,l] &= \frac{1}{\sqrt{N}}\sum_{m=0}^{N-1} y[k,m]e^{-\jmath 2\pi\frac{ml}{N}} \\ &= a_{k,l}e^{\jmath\phi}e^{-\jmath 2\pi\frac{\tau_k l}{T}} + W[k,l]. \end{aligned} \tag{9}$$

The Fourier transform of the Gaussian white noise $w[k,m]$ is $W[k,l]$. The samples of both forms are independent and identically distributed random variables and their variance is σ_w^2.

The demodulated base band echo $Y[k,l]$ is analysed to estimate the range of the target. Different filters can be used to this end, among which the matched filter (MF) and the zero forcing filter (ZF).

A) Matched filter

The matched filter estimates the spectral density of the echo by multiplying it by $\overline{a}_{k,l}$, the conjugate of the complex symbol $a_{k,l}$. An inverse Fourier transform results in a correlation function with a peak at the delay of the target. The k^{th} range profile is [3]

$$\begin{aligned} \chi[i] &= \frac{e^{\jmath\phi}}{\sqrt{N}}\sum_{l=0}^{N-1} Y[k,l]\overline{a}_{k,l}e^{\jmath 2\pi\frac{li}{N}} \\ &= \frac{e^{\jmath\phi}}{\sqrt{N}}\sum_{l=0}^{N-1} |a_{k,l}|^2 e^{\jmath\frac{2\pi}{N}\left(i-\frac{N\tau_k}{T}\right)l} \\ &\quad + \frac{e^{\jmath\phi}}{\sqrt{N}}\sum_{l=0}^{N-1} W[k,l]\overline{a}_{k,l}e^{\jmath 2\pi\frac{li}{N}}. \end{aligned} \tag{10}$$

Assuming that the delay τ_k is such that $i_k = \frac{\tau_k N}{T}$ is integer, the peak is then

$$\begin{aligned} \chi[i_k] = &\frac{e^{\jmath\phi}}{\sqrt{N}}\sum_{l=0}^{N-1} |a_{k,l}|^2 \\ &+ \frac{1}{\sqrt{N}}\sum_{l=0}^{N-1} W[k,l]\overline{a}_{k,l}e^{\jmath\phi}e^{\jmath 2\pi\frac{li}{N}}. \end{aligned} \tag{11}$$

Note that in the off-grid scenario (where i_k is not an integer), a spectrum leakage controlling window such as Chebyshev is needed for (11) to be valid, taking into account the Chebyshev window characteristics.

Knowing that $E[W[k,l]] = 0$, the magnitude of the first moment of the range profile is, for all i

$$|E[\chi[i]]| = \frac{1}{\sqrt{N}}\left|\sum_{l=0}^{N-1} |a_{k,l}|^2 e^{\jmath\frac{2\pi}{N}\left(i-\frac{N\tau_k}{T}\right)l}\right|. \tag{12}$$

The magnitude of the first moment of the main lobe is

$$\begin{aligned} |E[\chi[i_k]]| &= \frac{1}{\sqrt{N}}\sum_{l=0}^{N-1} |a_{k,l}|^2 \\ &= \sqrt{N}\sigma_a^2, \end{aligned} \tag{13}$$

with σ_a^2 the variance of $a_{k,l}$. It is assumed that N is large enough to verify $\lim\limits_{N\to+\infty}\sum\limits_{l=0}^{N-1}|a_{k,l}|^2 = N\sigma_a^2$. However, this first approximation is not tight enough, as shown in [6]. We then need to use the second order.

Since the data samples $a_{k,l}$ and the noise samples $W[k,l]$ are mutually independant, the second moment of the range profile is

$$E\left[|\chi[i]|^2\right] = |E[\chi[i]]|^2 + \sigma_a^2\sigma_w^2. \tag{14}$$

Thus, the average intensity of the range profile for a matched filter OFDM radar is

$$E\left[|\chi[i]|^2\right] = \frac{1}{N}\left|\sum_{l=0}^{N-1} |a_{k,l}|^2 e^{\jmath\frac{2\pi}{N}\left(i-\frac{N\tau_k}{T}\right)l}\right|^2 + \sigma_a^2\sigma_w^2 \tag{15}$$

and the second order of the main lobe is

$$E\left[|\chi[i_k]|^2\right] = \frac{1}{N}\left|\sum_{l=0}^{N-1}|a_{k,l}|^2\right|^2 + \sigma_a^2\sigma_w^2$$
$$= \frac{1}{N}\sum_{l=0}^{N-1}|a_{k,l}|^4 + \frac{1}{N}\sum_{l=0}^{N-1}\sum_{\substack{l'=0\\l'\neq l}}^{N-1}|a_{k,l}|^2|a_{k,l'}|^2 + \sigma_a^2\sigma_w^2$$
$$= \mu_a^4 + (N-1)\sigma_a^4 + \sigma_a^2\sigma_w^2, \quad (16)$$

assuming N is large enough such that $\mu_a^4 = E[|a_{k,l}|^4]$.

B) Zero forcing

The zero forcing filter (ZF) estimates the transfer function of the channel through an elementwise division [4]. An inverse Fourier transform gives the impulse response with a peak at the delay of the target. The k^{th} range profile is

$$\chi[i] = \frac{e^{\jmath\phi}}{\sqrt{N}}\sum_{l=0}^{N-1}\frac{Y[k,l]}{a_{k,l}}e^{\jmath 2\pi\frac{li}{N}}$$
$$= \frac{e^{\jmath\phi}}{\sqrt{N}}\sum_{l=0}^{N-1}e^{\jmath\frac{2\pi}{N}\left(i-\frac{N\tau_k}{T}\right)l}$$
$$+ \frac{e^{\jmath\phi}}{\sqrt{N}}\sum_{l=0}^{N-1}\frac{W[k,l]}{a_{k,l}}e^{\jmath 2\pi\frac{li}{N}}. \quad (17)$$

The magnitude of the first moment of the range profile is

$$|E[\chi[i]]| = \frac{1}{\sqrt{N}}\left|\sum_{l=0}^{N-1}e^{\jmath\frac{2\pi}{N}\left(i-\frac{N\tau_k}{T}\right)l}\right| = \sqrt{N}\mathbb{1}(i=i_k), \quad (18)$$

where $\mathbb{1}(i=i_k)$ is the indicator function that equals 1 when $i=i_k$ and equals zero otherwise. Again for more accuracy, we need to use the second order. The second moment of the range profile is

$$E\left[|\chi[i]|^2\right] = |E[\chi[i]]|^2 + \frac{1}{\sqrt{N}}\sum_{l=0}^{N-1}\frac{\sigma_w^2}{|a_{k,l}|^2}$$
$$= |E[\chi[i]]|^2 + \sigma_{1/a}^2\sigma_w^2, \quad (19)$$

where $\sigma_{1/a}^2$ is the average of $\frac{1}{|a_{k,l}|^2}$. Finally, the average intensity of the range profile for a zero forcing filter OFDM radar is

$$E\left[|\chi[i]|^2\right] = \frac{1}{N}\left|\sum_{l=0}^{N-1}e^{\jmath\frac{2\pi}{N}\left(i-\frac{N\tau_k}{T}\right)l}\right|^2 + \sigma_{1/a}^2\sigma_w^2 \quad (20)$$

and the second moment of the main lobe is

$$E\left[|\chi[i_k]|^2\right] = N + \sigma_{1/a}^2\sigma_w^2. \quad (21)$$

Now that the range profiles for OFDM/MF and OFDM/ZF have been decribed through their average intensity in (15) and (20), and the average intensity of their main lobe in (16) and (21), they can be compared via their PSLR and ISLR.

C) Peak to sidelobe ratio and integrated sidelobe ratio

The two metrics chosen for the comparison are PSLR and ISLR. The PSLR the ratio of the power of the main lobe to the power of the highest sidelobe. A bad PSLR means that there is a sidelobe so high that is could pass the threshold and trigger a false alarm. The ISLR, on the other hand, is the ratio of the integrated main lobe to the integrated sidelobes. A bad ISLR means that the main lobe could be below the threshold causing a miss detection.

Let γ be such as

$$\gamma^2 = E\left[\frac{|\chi[i_k]|^2}{\theta\left(\{|\chi[i]|^2\}_{i\neq i_k}\right)}\right], \quad (22)$$

with $\theta(\{x_i\}) = \max_i x_i$ for PSLR and $\theta(\{x_i\}) = \sum_i x_i$ for ISLR. Using the Jensen's inequality, the expectation of a ratio is approximate by the ratio of the expectations. The expression (22) becomes

$$\gamma^2 = \frac{E\left[|\chi[i_k]|^2\right]}{E\left[\theta\left(\{|\chi[i]|^2\}_{i\neq i_k}\right)\right]}. \quad (23)$$

Since the sampling rate is the nominal frequency, the main lobe is one sample wide. To evaluate γ^2 it remains to calculate the sum in (15) and (20). To this end, let $z[i] = e^{\jmath 2\pi\left(\frac{i}{N}-\frac{\tau_k}{T}\right)}$. The ratio for the MF filter is

$$\gamma_{\text{MF}}^2 = \frac{\mu_a^4 + (N-1)\sigma_a^4 + \sigma_w^2\sigma_a^2}{\theta\left(\left\{\frac{1}{N}\left|\sum_{l=0}^{N-1}|a_{k,l}|^2 z[i]^l\right|^2 + \sigma_w^2\sigma_a^2\right\}_{i\neq i_k}\right)} \quad (24)$$

and the ratio for a ZF filter is

$$\gamma_{\text{ZF}}^2 = \frac{N + \sigma_w^2\sigma_{1/a}^2}{\theta\left(\left\{\frac{1}{N}\left|\sum_{l=0}^{N-1}z[i]^l\right|^2 + \sigma_w^2\sigma_{1/a}^2\right\}_{i\neq i_k}\right)}. \quad (25)$$

Since $|z[i]| = 1$ for all i and by approximating the sum in (24) by its average with respect to $a_{k,l}$, it comes

$$E_a\left[\left|\sum_{l=0}^{N-1}|a_{k,l}|^2 z[i]^l\right|^2\right]$$
$$= N\mu_a^4 + \sum_{l=0}^{N-1}\sigma_a^2 z[i]^l\left(\sum_{\substack{l'=0\\l'\neq l}}^{N-1}\sigma_a^2 z[i]^{-l'}\right)$$
$$= N\mu_a^4 + \sigma_a^4\sum_{l=0}^{N-1}\left(\sum_{l'=0}^{N-1}z[i]^{l-l'} - 1\right)$$
$$= N(\mu_a^4 - \sigma_a^4) + \sigma_a^4\left|\sum_{l=0}^{N-1}z[i]^l\right|^2 \quad (26)$$

and

$$\gamma^2_{\text{MF}} = \frac{\mu_a^4 + (N-1)\sigma_a^4 + \sigma_w^2\sigma_a^2}{\theta\left(\left\{\frac{\sigma_a^4}{N}\left|\sum_{l=0}^{N-1} z[i]^l\right|^2 + \mu_a^4 - \sigma_a^4 + \sigma_w^2\sigma_a^2\right\}_{i\neq i_k}\right)}. \tag{27}$$

From this point and on, the θ function is approximated by its linear development, $\theta(x) = \eta x$. Using (20) and (27), the relationship between the ZF and the MF is obtained

$$\gamma^2_{\text{MF}} = \frac{1 + \frac{N\sigma_a^4}{\mu_a^4 - \sigma_a^4 + \sigma_w^2\sigma_a^2}}{1 + \frac{N}{\sigma_w^2\sigma_{1/a}^2}}\gamma^2_{\text{ZF}}, \tag{28}$$

for both the PSLR and the ISLR.

In low noise environments where $\sigma_w^2 \to 0$, $\gamma^2_{\text{MF}} < \gamma^2_{\text{ZF}}$ and, more specifically, this happens when

$$\sigma_w^2 < \frac{\mu_a^4 - \sigma_a^4}{\sigma_{1/a}^2 - \sigma_a^2}. \tag{29}$$

This can be written as

$$\text{SNR} = \frac{\sigma_a^2}{\sigma_w^2} > \frac{\frac{\sigma_{1/a}^2}{\sigma_a^2} - 1}{\frac{\mu_a^4}{\sigma_a^4} - 1}. \tag{30}$$

It is proposed that, in these low noise environments or high SNR regimes, ZF provides higher PSLR and ISLR compared to MF.

III. EXTENSION TO MMSE FILTER

The MMSE filter used here is the one applied to multi-carrier spread spectrum systems [7, § 2.1.5.1]. This filter minimizes the mean squared error between the transmitted symbols and the received ones. Applied to the range profile, it leads to

$$\begin{aligned}\chi[i] &= \frac{e^{\jmath\phi}}{\sqrt{N}}\sum_{l=0}^{N-1} Y[k,l]\frac{\overline{a}_{k,l}}{|a_{k,l}|^2 + \sigma_w^2}e^{\jmath 2\pi\frac{li}{N}} \\ &= \frac{e^{\jmath\phi}}{\sqrt{N}}\sum_{l=0}^{N-1}\frac{|a_{k,l}|^2}{|a_{k,l}|^2 + \sigma_w^2}e^{\jmath\frac{2\pi}{N}\left(i - \frac{N\tau_k}{T}\right)l} \\ &\quad + \frac{e^{\jmath\phi}}{\sqrt{N}}\sum_{l=0}^{N-1} W[k,l]\frac{\overline{a}_{k,l}}{|a_{k,l}|^2 + \sigma_w^2}e^{\jmath 2\pi\frac{li}{N}}. \end{aligned} \tag{31}$$

The same derivations as the ones used for the MF filter in II.A) are now followed. The second order moment of (31) follows the same logic as (14) and it is

$$E[|\chi[i])|^2] = |E[\chi[i]]|^2 + \sigma_w^2\sigma_c^2, \tag{32}$$

with $\sigma_c^2 = E\left[\frac{|a_{k,l}|^2}{(|a_{k,l}|^2+\sigma_w^2)^2}\right]$, and

$$|E[\chi[i]]|^2 = \frac{1}{N}\left|\sum_{l=0}^{N-1}\frac{|a_{k,l}|^2}{|a_{k,l}|^2 + \sigma_w^2}z[i]^l\right|^2. \tag{33}$$

All that is left is to replace $|a_{k,l}|^2$ in (26) by $\frac{|a_{k,l}|^2}{|a_{k,l}|^2+\sigma_w^2}$, and finally

$$\gamma^2_{\text{MMSE}} = \frac{1 + \frac{N\sigma_b^4}{\mu_b^4 - \sigma_b^4 + \sigma_w^2\sigma_c^2}}{1 + \frac{N}{\sigma_w^2\sigma_{1/a}^2}}\gamma^2_{\text{ZF}}, \tag{34}$$

where $\sigma_b^2 = E\left[\frac{|a_{k,l}|^2}{|a_{k,l}|^2+\sigma_w^2}\right]$ and $\mu_b^4 = E\left[\left(\frac{|a_{k,l}|^2}{|a_{k,l}|^2+\sigma_w^2}\right)^2\right]$. This relationship applies for both PSLR and ISLR. Contrary to the MF and ZF parameters, μ_a^4 or $\sigma_{1/a}^2$, the MMSE parameters μ_b^4, σ_b^2 and σ_c^2 depend on the noise level, which make it more difficult to predict trends in medium to high noise environments. When $\sigma_w^2 = 0$, the MMSE parameters are $\sigma_b^2 = \mu_b^4 = 1$ and $\sigma_c^2 = \sigma_{1/a}^2$. Thus, the MMSE equals the ZF in low noise environment.

Both expressions (28) and (34) are summarised in only one expression

$$\gamma^2 = \frac{1 + \frac{N\alpha}{\beta - \alpha + \sigma_w^2\delta}}{1 + \frac{N}{\sigma_w^2\sigma_{1/a}^2}}\gamma^2_{\text{ZF}}, \tag{35}$$

with α, β and δ given in table 1 for each MF and MMSE metrics.

Table 1. Metric parameters in (35).

	MF	MMSE
α	δ^2	$E\left[\frac{\lvert a_{k,l}\rvert^2}{\lvert a_{k,l}\rvert^2+\sigma_w^2}\right]$
β	$E[\lvert a_{k,l}\rvert^4]$	$E\left[\frac{\lvert a_{k,l}\rvert^4}{(\lvert a_{k,l}\rvert^2+\sigma_w^2)^2}\right]$
δ	$E[\lvert a_{k,l}\rvert^2]$	$E\left[\frac{\lvert a_{k,l}\rvert^2}{(\lvert a_{k,l}\rvert^2+\sigma_w^2)^2}\right]$

IV. RESULTS AND DISCUSSION

Simulations are performed to validate the expressions given by (28) and (34). Complex 16-QAM data symboles are carried on $N = 1024$ orthogonal subcarriers spanning a band of $B = 375$ MHz. The subcarrier spacing is 360 kHz and the OFDM symbol duration is $T = 2.73$ µs. The center frequency is $f_c = 77$ GHz. The duration of the cyclic prefix is the eighth of the duration of a symbol, $T_g = 0.34$ µs. This duration is enough for the sampling window of the

Table 2. OFDM radar parameters.

Parameter	Notation	Value
Number of sub-carriers	N	1024
Cyclic prefix	T_g	0.34 µs
Bandwidth	B	375 MHz
Order of QAM modulation	16-QAM	
Signal to noise power ratio	SNR $= \frac{\sigma_a^2}{\sigma_w^2}$	20 dB
Carrier frequency	f_c	77 GHz
Target distance	R	12 m

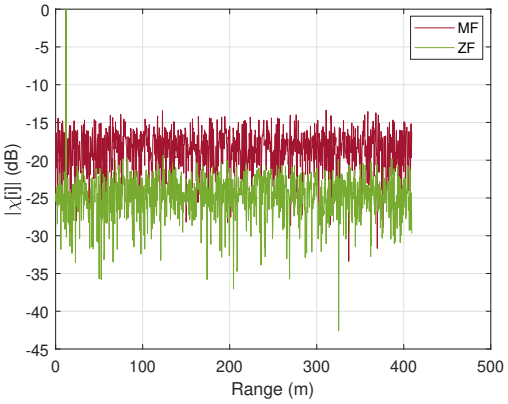

Fig. 1. Normalized and superimposed MF and ZF range profiles.

receiver end to include a whole symbol for target ranges under 50 m. The target range is $R = 12$ m which causes an integer delay. This allows us to go without the use of a Chebyshev window. The OFDM radar parameters for the simulation are summarized in table 2.

Range profiles are estimated through MF, ZF and MMSE using (10), (17) and (31), respectively. Then (22) is used to estimate the simulated γ_{PSLR} and γ_{ISLR} for each filter. The MF and MMSE performances obtained by simulation are compared to the MF and MMSE performances obtained with (28) and (34), respectively, and using the ZF performances obtained by simulation.

The normalized range profiles are shown superimposed in figure 1. The figure shows that, for SNR $= 20$ dB, MF exhibits higher sidelobes. Note that since MMSE is close to ZF in high SNR environments, it is not plotted here for clarity sake. These results confirm the proposition that in low noise environments, ZF and MMSE have higher PSLR and ISLR compared to MF. Next, the γ_{PSLR} and γ_{ISLR} are estimated for different SNR levels and the results are compared to the proposed expressions. The SNR is the ratio of the symbol power σ_a^2 to the noise power σ_w^2.

The plots show three main trends. In the high end of SNR, where SNR > 10 dB, (28) is proven to be accurate, since ZF shows a higher level of PSLR and ISLR, while MF plateaus. MMSE exhibits a behavior similar to that of a ZF filter as well as its performances. The expression (35) also proves true. For lower SNR between -20 and 10 dB, the noise is too high for (28) to apply. There, MF displays a slightly higher level or PSLR and ISLR. MMSE behaves more like an MF and (35) proves less accurate than

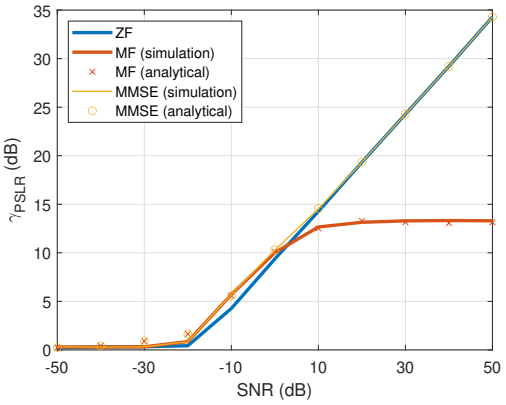

Fig. 2. PSLR versus input SNR.

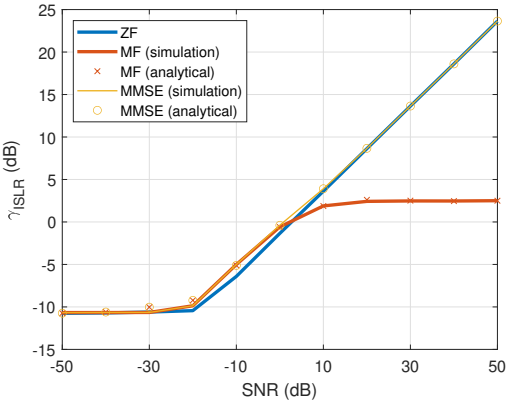

Fig. 3. ISLR versus input SNR.

in higher SNR environments. When the SNR < -30 dB, the noise level is too high for detection.

The main reason that could explain this difference in low-noise environments is the sidelobes due to the correlation function. Even when the noise level is low, these sidelobes remain unchanged, forcing the PSLR and ISLR in OFDM/MF radar to plateau. Whereas, the noise floor of an impulse response depends on the noise only.

A few assumptions or approximations are used to obtain the analytical performances: the asymptotic regime with large N, the Jensen's inequality for the PSLR and ISLR ratios in (23), the average in (26) and the linear development of θ. All these approximations are tight enough to get simple and efficient analytical expressions, as the simulation results show. Figure 4 shows the PSLR versus the number of subcarriers N in both a low noise environment (SNR $= 30$ dB) and a high noise environment (SNR $= -10$ dB). It shows that the expressions are accurate regardless of N.

However, when $\tau(t) \neq \tau_k$ through the payload time of the k^{th} echo, i.e. the variation of $\tau(t)$ during this time interval can not be neglected, the Doppler shift mismatches the filter by distorting the received signal. The stop-and-go approximation in (8) is not more valid and new derivations are needed. As shown in figure 5, MF is more

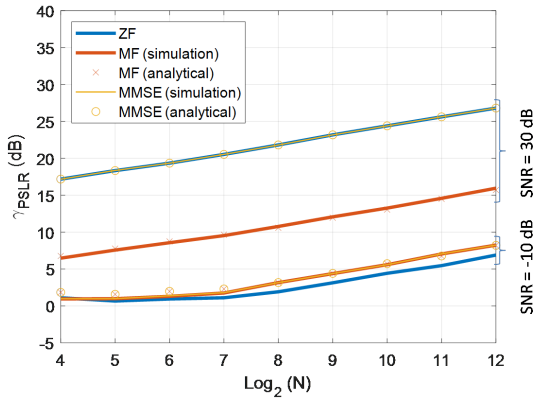

Fig. 4. PSLR versus N, SNR $\in \{-10, 30\}$ dB.

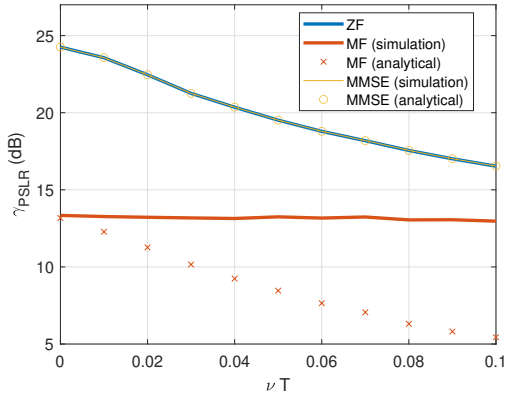

Fig. 5. PSLR versus Doppler shift, SNR $= 30$ dB.

robust to this mismatch than ZF: the performance of MF decreases slowly with the Doppler shift in contrast with ZF and MMSE ones. Due to this difference in behaviour, the analytical expression (28) is not valid in high SNR environments and significant Doppler. Note that a relative Doppler shift $\nu T = 0.1$ corresponds to a radial speed around 260 km/h, with $\nu = \frac{2vf_c}{c}$. Contrary to MF, the analytical MMSE performance matches the simulation one, and (34) remains valid for all Doppler shift conditions. In lower SNR regimes (see figure 6) the analytical derivations are valid for ZF and MMSE for all Doppler shifts.

V. CONCLUSION

In this paper, the OFDM radar filters used to estimate the range of the target are compared through the PSLR and ISLR of their range profiles. These filters are MF, ZF and MMSE. First MF and ZF are compared in different levels of noise. The performance of MF is derived from that of the ZF through an expression that is applicable to both PSLR and ISLR and that only depends on the modulation parameters. It is also found that, in low noise environments and with the assumption that the number of subcarriers is large enough, ZF performs better than MF. The analysis is then

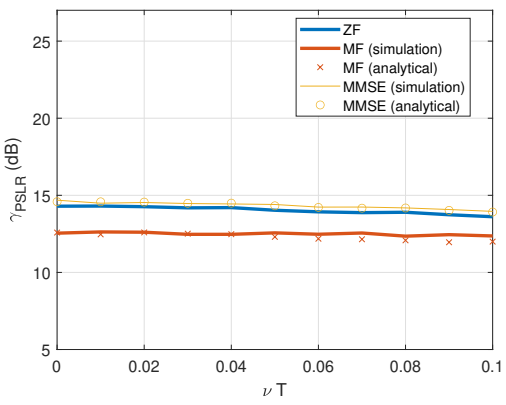

Fig. 6. PSLR versus Doppler shift, SNR $= 10$ dB.

extended to the MMSE filter. The MMSE filter behaves like a ZF in low noise environments and like an MF in high noise environments. The performance of MMSE is derived from that of the ZF through an expression that is applicable to both PSLR and ISLR and that only depends on the modulation parameters. The expression on MF and MMSE through ZF are verified by simulations.

ACKNOWLEDGMENT

The study has been partially funded by the French ANRT through the Cifre contract number 2019/0964.

REFERENCES

[1] Bourdoux, A., Parashar, K., Bauduin, M.: Phenomenology of mutual interference of FMCW and PMCW automotive radars. In 2017 IEEE Radar Conference (RadarConf) (pp. 1709-1714).

[2] Nguyen, T. T. (2012). Design and Analysis of Superresolution algorithm and signal separation technique for an OFDM-based MIMO radar (Master's thesis, Universitat Politècnica de Catalunya).

[3] Sen, S., Nehorai, A. (2009). Adaptive design of OFDM radar signal with improved wideband ambiguity function. IEEE Transactions on Signal Processing, 58(2), 928-933.

[4] Sturm, C., Pancera, E., Zwick, T., Wiesbeck, W. (2009, May). A novel approach to OFDM radar processing. In 2019 IEEE Radar Conference (pp. 1-4).

[5] Van Thillo, W., Gioffré, P., Giannini, V., Guermandi, D., Brebels, S., Bourdoux, A. (2013, October). Almost perfect auto-correlation sequences for binary phase-modulated continuous wave radar. In 2013 European Radar Conference (pp. 491-494).

[6] Benmeziane, B., Baudais, J.-Y., Méric, S., Cinglant, K. (2022, April). Comparison of ZF and MF filters through PSLR and ISLR assessment in automotive OFDM radar. In 2021 18th European Radar Conference (EuRAD) (pp. 193-196). IEEE.

[7] Fazel, K. and Kaiser, S., "Multi-carrier and spread spectrum techniques (From OFDM and MC-CDMA to LTE and WiMAX)", John Wiley & Sons Ltd, 2008

[8] Hakobyan, G. (2018). Orthogonal frequency division multiplexing multiple-input multiple-output automotive radar with novel signal processing algorithms.